Effect of Winding Speed on the Physical Structure of As-Spun Poly(ethylene Terephthalate) Fibers, Including Orientation-Induced Crystallization

H. M. HEUVEL and R. HUISMAN, *Akzo Research Laboratories Arnhem, Fibre Research Department, The Netherlands*

Synopsis

As-spun fibers of poly(ethylene terephthalate), PET, made at winding speeds ranging from 2000 to 6000 m/min exhibit quite different physical structures. Yarns wound at relatively low speeds are amorphous, whereas those spun at high speeds contain well-developed crystals of closely packed molecules. In this study the structures have been characterized by means of various techniques such as differential scanning calorimetry, x-ray diffraction, density, and pulse propagation measurements. Based on the results obtained, an arrangement of the molecules in the various yarns is proposed. It is shown that these arrangements can account for the extreme wide variety in contraction behavior found experimentally. Finally, the results obtained are compared with those of other investigations into orientation-induced crystallization.

INTRODUCTION

Studies of the crystalline structures formed during the melt spinning process were already reported before. Most of the work, however, was confined to the study of polyolefins, especially polyethylene and polypropylene.[1,2] Until now hardly any indication of a crystalline structure formed during spinning of PET fibers has been found in the literature. Wasiak and Ziabicki[3] investigated as-spun PET fibers wound at speeds ranging from 350 to 850 m/min and found the yarns to be amorphous. In an excellent paper Liska[4] describes his investigations into the molecular arrangements in undrawn PET yarns. The range of winding speeds involved was 1450 to 4000 m/min. In this range the transition from a- to c-axis orientation is found in the yarns after annealing. In the unannealed as-spun filaments of normal viscosity ($\eta_{sp} = 0.74$) no distinct crystalline structures were found. The highest winding speed, however, used for spinning a filament of higher viscosity ($\eta_{sp} = 0.88$) gave rise to an x-ray pattern with reflections evidently brought about by crystalline material. This crystal structure was not discussed in any detail.

The present study comprises winding speeds from 2000 to 6000 m/min. For the structure analysis different kinds of measurement were applied and elaborated as quantitatively as possible in order to make full profit of the combination of techniques. It was found that, at the spinning conditions used, distinct crystalline structures formed at winding speeds higher than 4000 m/min. From the study of these crystals it appeared that the stacking of the molecules in the crystal lattice, the sizes of the crystals, and their orientation depend on the winding speed. The same holds for the orientation of the molecules in the amorphous regions. So, in this paper the emphasis is on the description of physical structures ranging from quite amorphous to well-developed crystalline.

Journal of Applied Polymer Science, Vol. 22, 2229–2243 (1978)

0021-8995/78/0022-2229$01.00

A comparison of our results with those obtained in other investigations concerning strain-induced crystallization shows that the crystallization process involved is evidently orientation induced.

EXPERIMENTAL

The fibers were spun at a constant count of $d$tex 167 f 30. The spinning temperature used was 290°C and the diameter of the capillaries, 250 μm. The winding speeds were 2000, 2500, 3000, 3500, 4000, 4250, 4500, 4750, 5000, 5500, and 6000 m/min. In order to keep the count of the as-spun fibers constant, the flow rate was varied from 1.11 g/min at 2000 m/min to 3.34 g/min at 6000 m/min per single spinneret orifice.

The specific viscosity was 0.63 measured as a solution of 1 g PET in 100 g m-cresol at 25°C.

For the structure analysis the following techniques and instruments have been used:

Density. Density gradient column of Davenport, filled with a mixture of tetrachloromethane/n-heptane at 23°C.

Differential Thermal Analysis. du Pont 990 TA with a cell base operating with a DSC cell at a heating rate of 20°C/min.

Pulse Propagation. Dynamic modulus tester PPM-5 of H. Morgan Co. (Cambridge, Mass.) at a tension of 2 cN/tex.

Thermomechanical Analysis. TMS-1 of Perkin-Elmer, using a heating rate of 20°C/min at a starting load of 0.04 cN/tex. During this kind of contraction experiments the load has basically to be kept constant. Because of the low load needed and the large contractions involved, this requirement could not be met. In practice the load increases at increasing contraction caused by the buoyancy of the floating system not being constant. For the purpose of qualitative interpretation as discussed further on in this paper, this effect is of no importance, however.

X-Ray Diffraction. The WAXS work was carried out with a Philips diffractometer provided with a quartz monochromator, Soller slits, a divergence slit (1°), a scatter slit (0.2 mm), and a receiving slit (1°). The diffractometer was directly coupled to a Hewlett-Packard counter and paper tape device for further quantitative elaboration. Use was made of the transmission technique, resulting in symmetrical diffraction profiles[5] as required for the computer simulation applied. The SAXS experiments were made in a Kiessig camera.

Calculations were performed on a CDC 6600 and a Harris slash 4 VMS computer.

RESULTS OF STRUCTURE ANALYSIS

The first quantity determined is the overall density d_4^{23}. The results of these measurements are presented in Figure 1, where the density is shown as a function of the winding speed. At a speed of 3500 m/min, the beginning of a sharp increase in the overall density can be seen. At the highest winding speeds a tendency toward saturation is observed.

In Figure 2 the DTA diagrams are given. First the two extreme situations of 2000 and 6000 m/min are considered. For the lower winding speed the glass

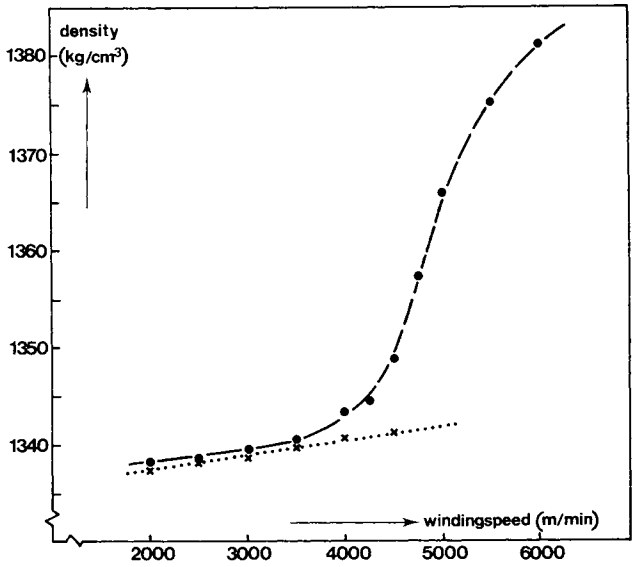

Fig. 1. (●) Experimental density as function of winding speed. (×) Calculated amorphous density depending on orientation.

transition can be seen at about 76°C, followed by the crystallization exotherm with a peak temperature near 132°C and after that a melting endotherm with its minimum at about 253°C. From this DTA trace it can be concluded that the original fiber wound at 2000 m/min is largely amorphous because the crystalline material that melts finally has formed during the DTA run as indicated by the crystallization peak. In sharp contrast to this DTA trace is the one brought about by the yarn wound at 6000 m/min. This curve only shows a melting endotherm, indicating that this material originally is already partially crystalline. The situations in between these two extremes show a gradual change. The glass transition is found at a constant temperature of 76°C up to winding speeds of about 4000 m/min. Also the crystallization exotherm is shown by the same group of yarns. Between 4000 and 5000 m/min, however, a sharp distinction between glass transition and crystallization exotherm can no longer be made. This is caused by the fact that the crystallization peak shifts gradually to lower temperatures at increasing winding speeds. At speeds above 5000 m/min no transition is observed any longer in the DTA diagrams except melting. Concerning the melting peaks it can be seen that at about 4000 m/min the shape of the melting peak starts to change. The rather broad peak found for the yarns wound at low speeds converts via mixed situations to a sharp one as found for the yarns taken up at the highest speeds.

Summarizing, it can be concluded from DTA measurements that the physical structure of as-spun PET fibers changes from amorphous to semicrystalline within the range of winding speeds investigated. Quantitative conclusions about the amount of crystallinities cannot be obtained from the DTA measurements because of the uncertainties with respect to the course of the baseline. The shape of the melting peak suggests that the yarns taken up at velocities higher than 4000 m/min contain some crystalline material originally. This coincides reasonably well with the onset of the sharp increase of the density described before.

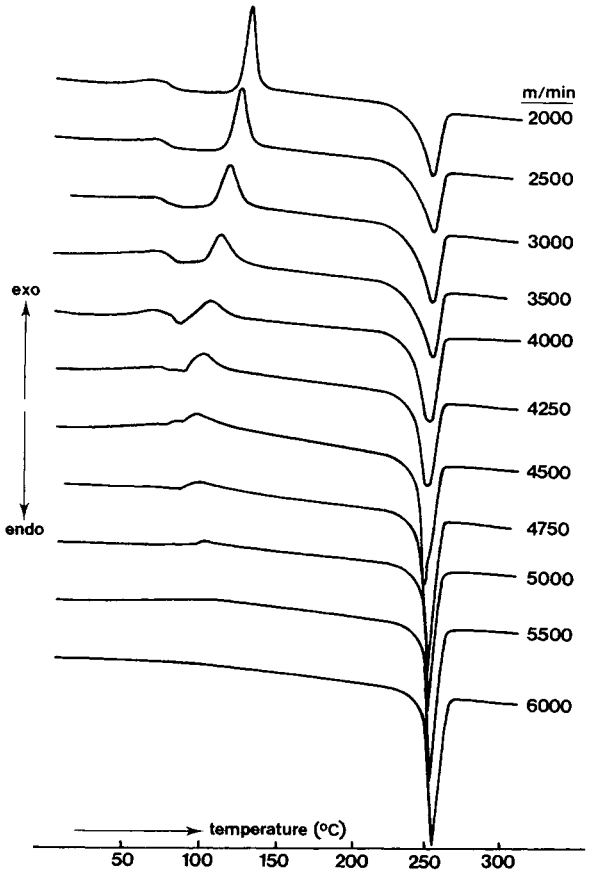

Fig. 2. DTA traces of yarns wound at the indicated velocities.

For a qualitative impression of the crystalline structures of the as-spun fibers involved, Astbury pictures were made. The most relevant photographs are shown in Figure 3. In the region of the lowest winding speeds only an amorphous halo can be seen. At increasing speeds this halo gradually concentrates toward the equator indicating an improved orientation of the molecules in the predominantly amorphous samples. The first indications of some very poorly developed crystalline material are visible in the picture of the yarn wound at 4500 m/min. The Astbury photographs of the yarns wound at even higher speeds show increasingly sharper spots pointing to a further developed crystalline material.

To obtain more detailed quantitative information various types of diffractometer scan have been made of the semicrystalline samples.

In Figure 4 the equatorial x-ray diffraction traces are given for the situations ranging from 4500 to 6000 m/min. The traces illustrate quite evidently the immense influence the winding speed has on the crystalline structure. For the yarns wound at high winding speeds well resolved patterns are found. The yarns taken up at lower speeds only give rise to broad unresolved traces. As, according to Scherrer's formula, narrow peaks are related to crystals which are large in the direction perpendicular to the crystal plane involved, it can be concluded that the lateral dimensions of the crystals in the yarns wound at high speeds are rel-

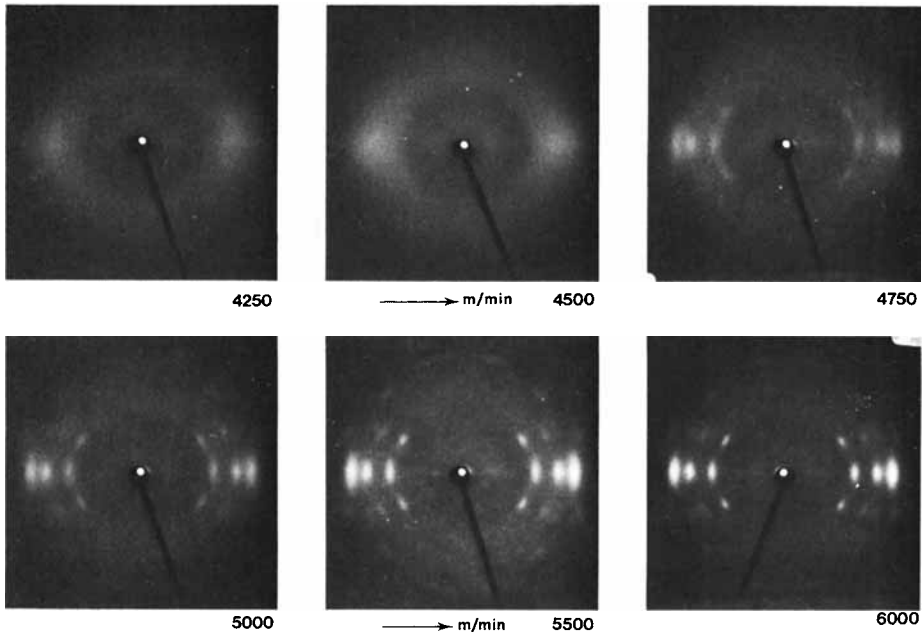

Fig. 3. Astbury pictures of yarns wound at the indicated speeds.

atively well developed. The fact that the intensity of the profiles increases with the winding speed does not provide additional information. This phenomenon may be caused by an improved orientation and/or a decrease of the half-widths of the peaks.

To derive quantitative information from the traces presented, the profiles have been fitted to the sum of three so-called Pearson VII curves. This procedure has been described in detail elsewhere.[6,7] Essential in this elaboration is that the Pearson VII formula is very versatile and can describe many types of symmetrical bell-shaped traces, including the Cauchy and Gauss profiles. For the iteration procedure it was found necessary to work with upper and lower limits for the parameters to be adjusted in order to reach convergence. This way of elaboration proved to provide accurate information about peak positions, half-widths, and intensities. Also the radial diffractometer scans of the $\bar{1}05$ reflections were made and computer fittings with one Pearson VII line calculated. The resulting peak positions were combined with the values obtained from the equatorial scans to calculate the axes of the unit cell. For these calculations the angles of the triclinic unit cell were assumed to be constant having the values $\alpha = 100.1°$, $\beta = 117.9°$, and $\gamma = 110.7°$.[7] Those results which could be obtained with sufficient reliability are given in Table I, together with the crystal sizes calculated from the observed half-widths of the peaks. The indications a and b refer to the axes of the basal plane of the unit cell as depicted in Figure 5. The height of the unit cell is indicated by c. The symbol Λ^*_{010} stands for the crystal thickness perpendicular to the a-axis; Λ^*_{100}, for the thickness perpendicular to the b-axis; and $\Lambda^*_{\bar{1}05}$, for the height of the crystal, all three quantities not being corrected for paracrystalline distortions as indicated by the asterisks.

From the unit cell dimensions the crystalline densities were also calculated and reported in Table I. From this table it can be seen that in general the lengths of the axes decrease at increasing winding speed. This fact has not only been

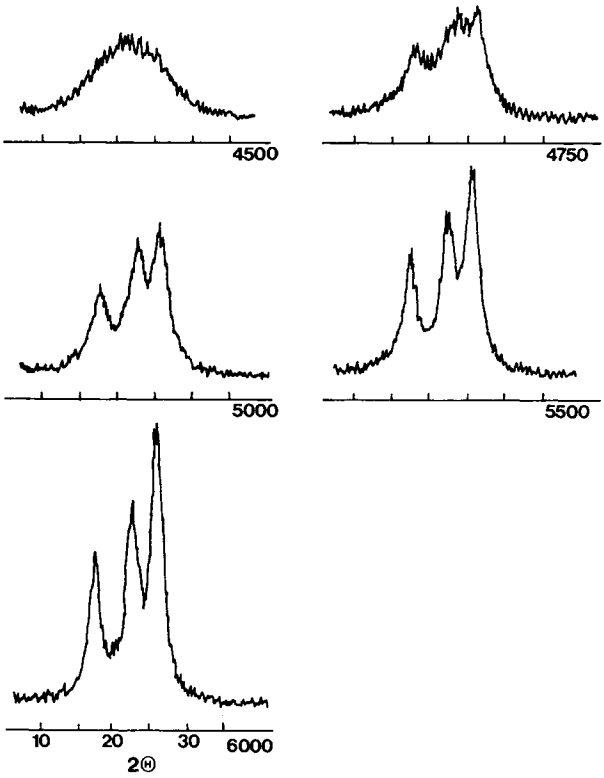

Fig. 4. Equatorial x-ray diffractometer scans.

found in this series but was confirmed in many other analogous investigations in this laboratory. The closer stacking of the molecules in the crystals of yarns taken up at higher speeds is most evidently illustrated by the behavior of the a-axis and the crystalline density. The observation that the a-axis is the most sensitive is not only caused by the fact that its value can be determined most accurately, but there is also a physical reason. The a-axis is along the exchange interaction between the π-electrons, whereas the b-axis is mainly in the direction of the stronger dipole–dipole interaction. According to other experiments,[7] apparently the interaction energy along the a-axis is of such order of magnitude that the temperature at which the crystal forms influences the stacking of the

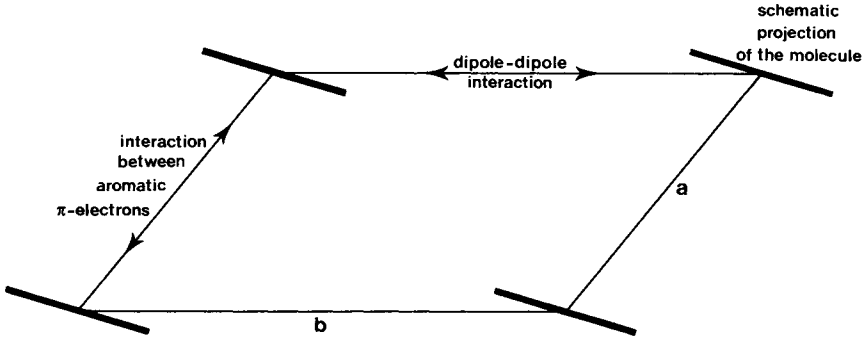

Fig. 5. Schematic basal plane of unit cell and representation of intermolecular interactions.

TABLE I
Results from Quantitative Elaboration of WAXS Experiments

Winding speed, m/min	Unit cell			Apparent crystal sizes			Crystalline density d_c, kg/m^3	Estimated crystallization temperature, °C
	Basal plane		Height	Lateral		Height		
	a, Å	b, Å	c, Å	$\Lambda^{\bullet}_{010}$, Å	$\Lambda^{\bullet}_{100}$, Å	$\Lambda^{\bullet}_{105}$, Å		
4750	4.504	5.90	10.72	24	29	54	1488	186
5000	4.495	5.88	10.72	29	34	57	1495	198
5500	4.485	5.88	10.71	41	41	76	1499	212
6000	4.480	5.88	10.71	51	49	84	1501	218

molecules in the direction of the a-axis. This finding has been used to estimate crystallization temperatures from the tabulated values of the a-axis for the various winding speeds. The estimated temperatures are given in Table I. Concerning the crystal sizes, it can be concluded that in all three dimensions the crystals are larger when formed at a higher winding speed. As confirmed in many other experiments carried out by us, the most pronounced lateral growth is in the direction of the strong dipole–dipole interaction, as indicated by Λ^*_{010} being more sensitive to the winding speed than Λ^*_{100}. In this way the energy is lowered in the most effective way during the crystallization process.

By making WAXS azimuthal scans the crystalline orientation was determined. For PET the most suitable reflection for this purpose is the $\bar{1}05$ reflection. Basically, these azimuthal traces consist of two identical $\bar{1}05$ peaks and two minor $0\bar{2}4$ peaks on the wings. The four contributions can be seen separately in the patterns brought about by the yarns wound at the highest speeds, as illustrated in Figure 6. The patterns shown were fitted with four Pearson VII lines, taking into account that both $\bar{1}05$ peaks and both $0\bar{2}4$ peaks have to be identical, with the centers of both pairs coinciding. In this way, for the unresolved profiles related to the yarns taken up at low speeds, good fittings and reliable parameter values could also be obtained. From the resulting parameters of the $\bar{1}05$ line the crystalline orientation factor f_c is calculated according to the method of Hermans et al.[8] The results are listed in Table II. It should be noted that already at the winding speed of 4750 m/min a very high, nearly saturated value is obtained.

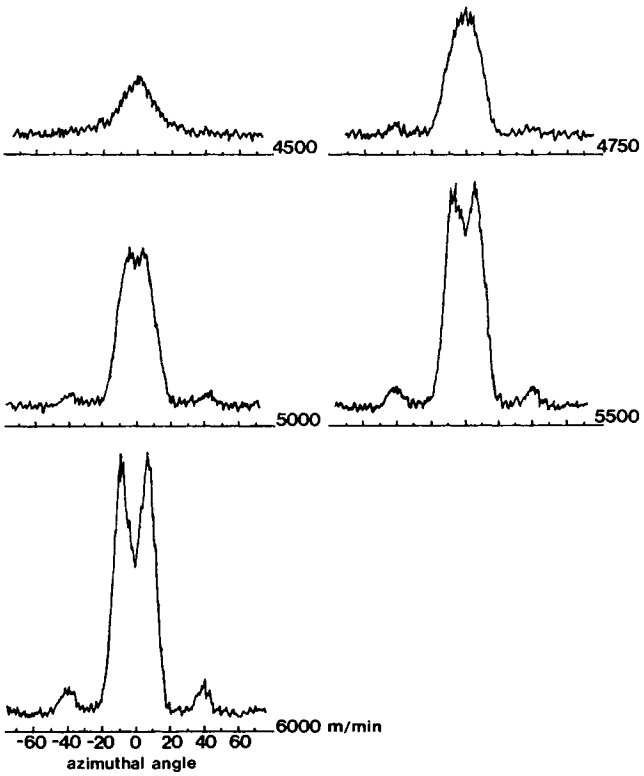

Fig. 6. Azimuthal x-ray diffractometer scans over the $\bar{1}05$ reflections.

TABLE II
Physical Quantities Related to Orientation

Winding speed, m/min	Sonic modulus, $(N/m^2) \times 10^{10}$	Crystalline orientation factor f_c	Amorphous orientation factor f_a	Volume fraction crystallinity
2000	0.301	—	0.093	0
2500	0.323	—	0.155	0
3000	0.362	—	0.246	0
3500	0.431	—	0.367	0
4000	0.543			
4250	0.600			
4500	0.691	0.76	(0.589)	(0.056)
4750	0.763	0.965	0.602	0.106
5000	0.857	0.972	0.626	0.155
5500	0.978	0.976	0.650	0.209
6000	1.160	0.979	0.693	0.242

To get an insight into the orientation of the molecules in the amorphous regions, these crystalline orientation factors must be combined with pulse propagation measurments. This technique provides the propagation velocity of longitudinal waves (freq. 10 kc/sec) in the yarns. During the measurements the yarns were loaded to a tension of 2 cN/tex. In a separate series of measurements it was established that within the range of 0.5–3.5 cN/tex the pulse propagation velocity was nearly insensitive to the tension applied. When the pulse propagation velocity is known, the sonic modulus can be calculated.[9] The values so obtained are listed in Table II and plotted in Figure 7 versus the winding speed. It can be seen that extrapolation to a winding speed of zero agrees with the value

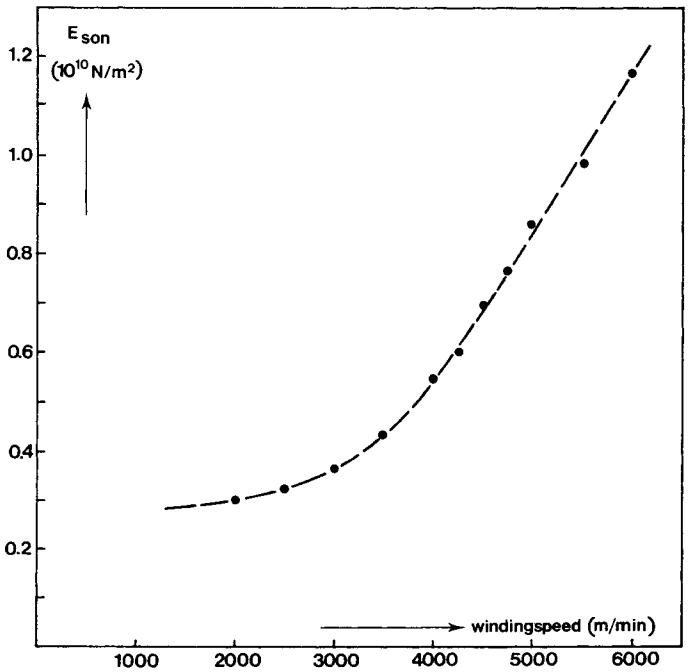

Fig. 7. Sonic modulus as function of winding speed.

of 0.273×10^{10} N/m^2 determined by Dumbleton[10] for unoriented amorphous samples.

To obtain amorphous orientation factors f_a these sonic moduli values have been combined with the crystalline orientation factors f_c, using the method proposed by Samuels[11] and elaborated by Dumbleton.[10] In order to use this method, values for the volume fraction of crystalline material, V_c, were needed. This quantity was calculated from the measured overall density d_4^{23}, the crystalline density d_c as calculated from x-ray diffraction measurements, and the amorphous density d_a. This last quantity depends to some extent on the amorphous orientation factor f_a.[7] The quantitative relation, established in a separate set of experiments, is

$$d_a = 1336 + 9.4 f_a \tag{1}$$

So, successive approximations were needed in the calculation of f_a. One starts, for example, with a value $d_a = 1336$ kg/m^3, calculates V_c, which can be used for the first approximation of f_a, which value is used in formula (1) to give a better approximation of d_a and hence of V_c, etc. This procedure converges very rapidly, and two or three successive approximations are sufficient to obtain consistent values of f_a and V_c. The results are reported in Table II. For the situation of the winding speed of 4500 m/min, an extrapolated value of the crystalline density of 1470 kg/m^3 was used for the calculations. The structure parameters obtained from the unresolved broad diffraction pattern involved were not accurate enough to enable the calculation of the crystalline density to be made with the precision required.

Relation (1) has also been used to calculate the density of the yarns, supposing that they are quite amorphous. The results are included in Figure 1. It can be seen that for the four lowest winding speeds a good agreement is obtained apart from a small difference in density level. For higher winding speeds the deviations increase rapidly. The observation clearly indicates that for these winding speeds also some crystalline material contributes to the overall density. This result agrees fairly well with the conclusion from DTA melting traces. Also the course of the volume fraction of crystalline material, plotted versus the winding speed as given in Figure 8, suggests that at 4000 or 4250 m/min the first contribution of crystalline material can be expected. So, the calculation of amorphous orientation factors, assuming $V_c = 0$, has been limited to the four lowest winding speeds. In Figure 9 both the crystalline and the amorphous orientation factors have been plotted versus the winding speeds. Striking is the rapid saturation of the crystalline orientation and the gradual course of the amorphous orientation.

SAXS experiments, carried out with the samples wound at the highest speeds, did not show any diffracted intensity. The reason for this finding is discussed further on in this paper.

SURVEY OF STRUCTURAL MODELS AND IMPLICATIONS FOR CONTRACTION BEHAVIOR

As a kind of qualitative summary of the findings presented before a rough picture can be made of the structures of the as-spun fibers as presented in Figure 10. At a winding speed of 2000 m/min a fiber is produced consisting of molecules

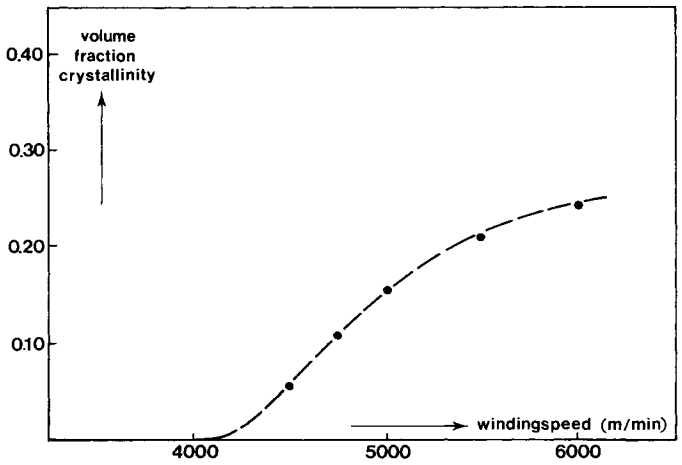

Fig. 8. Volume fraction crystallinity vs winding speed.

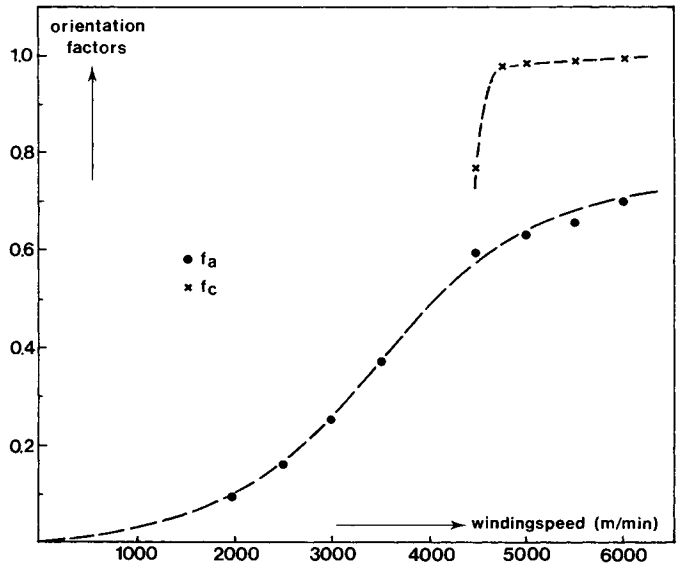

Fig. 9. Amorphous (●) and crystalline (×) orientation factors vs winding speed.

with low orientation which have not crystallized. An increase in winding speed up to 3500 m/min results only in an increased orientation without any indication of crystallization. At higher winding speeds some crystallization becomes apparent, while at speeds of 5000 m/min and higher, very well-developed crystals are detected.

These models account nicely for the extreme differences in mechanical properties in this series of as-spun fibers as illustrated by the contraction measurements shown in Figure 11. For the yarn wound at 2000 m/min only contraction in the glass transition region is found, pointing to a disorientation process in the amorphous material leading to an increased entropy. With further increase in temperature the modulus of the soft amorphous substance becomes so low that only elongation can take place. At 2500 m/min the amorphous material is better oriented, resulting in a higher contraction during disorientation

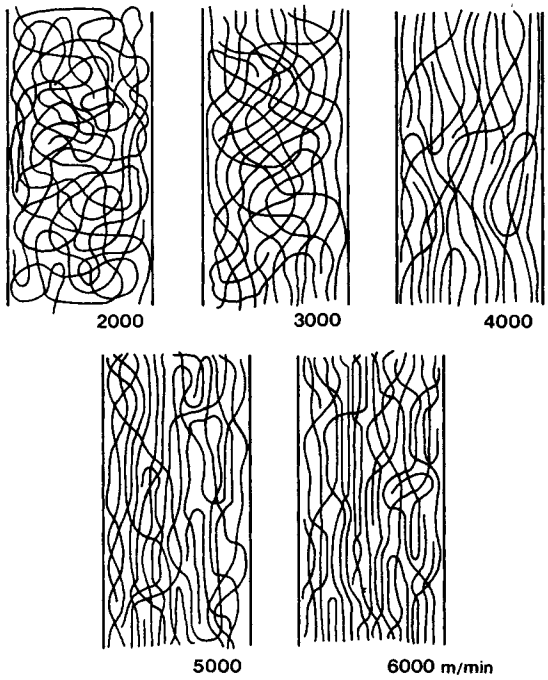

Fig. 10. Proposed molecular arrangements in yarns wound at various speeds.

after passing the glass transition temperature. In this case during the subsequent elongation some crystallization can already take place. This is in accordance with the DTA diagrams of Figure 2, which show that at higher winding speeds the crystallization shifts to lower temperatures.

This crystallization process, taking place during the TMA measurement, provides some physical crosslinks that prevent further elongation. The same effect can be seen at a further increase in winding speed: increasing contraction at the glass transition temperature caused by an increased orientation of the amorphous material, and a decreasing softening caused by the fact that the crystallization process comes closer to the glass transition region. At 4000 m/min the first decrease of contraction during the glass transition is observed. This can be ascribed to the forthcoming crystallization in the as-spun yarns as revealed in Figures 1 and 8. The increase in crystallinity as present in the original samples produces a very pronounced decrease of the glass transition contraction as illustrated by the TMS traces of samples wound at higher speeds. For these situations another contraction peak arises, viz., in the melting region. In this region the well-oriented crystalline domains melt and the released molecules will disorient in order to reach an increase in entropy. In this interpretation this peak has to depend on the crystallinity and the crystalline orientation. A comparison of the contraction experiments with both these quantities shown in Figure 11 is in fairly good agreement with this explanation.

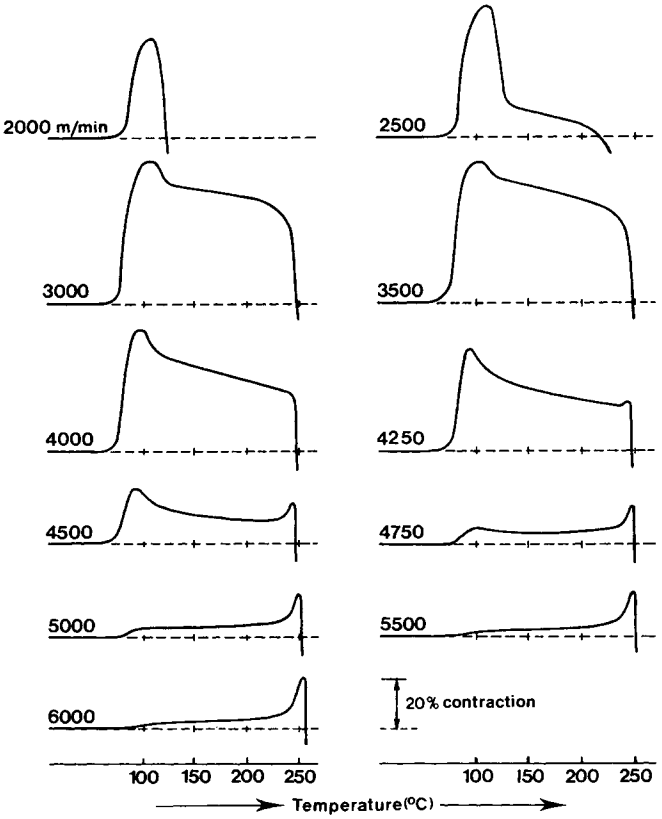

Fig. 11. Contraction as function of increasing temperature for yarns taken up at the indicated speeds.

ORIGIN OF CRYSTALLINE STRUCTURES IN THE AS-SPUN PET FIBERS

Many interesting papers have been published about crystallization under conditions of molecular orientation.[1,3,12–15] It was not the purpose of this investigation to study the crystallization mechanism as such, and hence we try only to compare our results with the ideas put forward in some papers referred to above.

First of all, it is very clear that the crystallization process during spinning at high winding speeds as described before is many decades faster than that found for PET crystallizing from the isotropic melt. This is in agreement with all findings of crystallization under conditions of molecular orientation. This fact is attributed generally to the reduced entropy gain during the melting of crystals under orientation conditions.[16] Consequently, the melting point increases when the released molecules are more restricted in their mobility. Considering a spinning fiber as a cooling melt, this implies that the supercooling at a given temperature is higher when more molecular orientation exists or, in other words, when the fiber is taken up at a higher winding speed. According to Peterlin,[15] the critical size of the primary crystallization nucleus decreases and the crystallization rate increases exponentially with the supercooling. From the first phenomenon it must be expected that the use of a high winding speed results

in a crystal structure formed at a high temperature. This is in accordance with the finding that the a-axis of the elementary cell is shorter for higher winding speeds indicating higher crystallization temperatures, as can be seen from Table I. The effect of the different degrees of supercooling on the crystallization rate accounts for the finding that the crystallinity increases with the take-up velocity above 4000 m/min. Below this winding speed no crystalline structure at all could be detected.

Nevertheless, also for the low winding speeds a definite influence of the orientation on the crystallization behavior can be seen. Wasiak and Ziabicki,[3] among others, found that the half-time of crystallization at 95°C was reduced when molecular orientation was improved. We saw the same kind of effect from the DTA diagrams presented in Figure 2. In these nonisothermal measurements the increased tendency to crystallization is reflected in a shift of the crystallization exotherms to lower temperatures at increased winding speeds. The shape of the DTA traces also suggests that the continuation of the crystallization process, when started at a lower temperature, is retarded. This is in accordance with the findings of Kawai et al.[12]

The fact that SAXS measurements carried out with samples wound at the highest speed did not show any diffracted intensity suggests that the crystallites formed during spinning are not predominantly of the folded chain type.[17] This point is under further investigation, especially with IR and thermal stress analysis. If the view mentioned is correct, the orientation-induced crystallization process involved has a more intermolecular character than the thermally induced process. The latter gives rise to folded-chain lamellae, as reported by Yeh,[14] and consequently is more intramolecular. The crystallites found in the as-spun yarns wound at speeds above 4000 m/min show all features mentioned by Yeh[14] describing the main characteristics of strain-induced crystallites. They have formed extremely fast; i.e., in a few milliseconds they are nearly perfectly oriented and their height does not exceed 100 Å. The course of the height (Λ^*_{105}) and the thickness (Λ^*_{010}) with the take-up velocity suggests that in the very short time available for crystallization no epitaxial overgrowth could take place. Both crystal dimensions have been found to increase with the winding speed (see Table I), whereas epitaxial overgrowth would give rise to a far more pronounced increase in thickness, the height remaining nearly constant. So this finding points in the same direction as the absence of SAXS intensity.

As already mentioned, it is thought that the molecular orientation is responsible for the spectacular change in crystallization behavior of spinning fibers when the take-up velocity is varied. Hence, said velocity is not the only spinning variable to influence this crystallization process. Other spinning conditions which may affect molecular orientation can also be used to direct the crystallization process. Liska[4] already found a first indication of the influence of the viscosity on the crystallization of PET at a winding speed of 4000 m/min. In this laboratory,[18] it has been established that an increase in the specific viscosity of the polymer by 0.1 corresponds with an increase in the winding speed of about 500 m/min, keeping the other spinning conditions constant. Other parameters which may influence molecular orientation, and hence the crystallization behavior, during spinning are spinning temperature, shape of the spinneret orifice, way of cooling the bundle, draw-down ratio, and yarn count, among others.

The authors gratefully acknowledge the following contributions to the work presented: H. J. E.

Oesterholt for spinning the yarns; Lenie Adolfsen, Marian Nijpjes, B. A. Schipper, L. J. Lucas, V. Bantwal Rao, and H. J. v.d. Ven for their experimental work on structure analysis; and M. Mannee for his help with the computer calculations. The cooperation with Dr. J. A. Juijn promoting technological experiments based on the ideas presented in this paper was very stimulating.

References

1. K. Katayama, T. Amano, and K. Nakamura, *Kolloid-Z.*, **226,** 125 (1968).
2. V. G. Baranov, T. I. Volkov, G. S. Farshyan, and S. Ya. Frenkel, *J. Polym. Sci. C,* **30,** 305 (1970).
3. A. Wasiak, and A. Ziabicki, *Appl. Polym. Symp.*, **27,** 111 (1975).
4. E. Liska, *Kolloid-Z.*, **251,** 1028 (1973).
5. L. E. Alexander, *X-Ray Diffraction Methods in Polymer Science,* Wiley-Interscience, New York, 1969, pp. 77–82.
6. H. M. Heuvel, R. Huisman, and K. C. J. B. Lind, *J. Polym. Sci., Polym. Phys. Ed.*, **14,** 921 (1976).
7. R. Huisman and H. M. Heuvel, *J. Appl. Polym. Sci.*, to appear.
8. J. J. Hermans, R. H. Hermans, D. Vermaas, and A. Weidinger, *Rec. Trav. Chim.*, **65,** 427 (1946).
9. J. W. Ballou and S. Silverman, *Text. Res. J.*, **14,** 282 (1944).
10. J. H. Dumbleton, *J. Polym. Sci. A-2,* **6,** 795 (1968).
11. R. J. Samuels, *J. Polym. Sci. A-2,* **3,** 1741 (1965).
12. T. Kawai, M. Iguchi, and H. Tonami, *Kolloid-Z.*, **221,** 28 (1967).
13. R. D. Ulrich and F. P. Price, *J. Appl. Polym. Sci.*, **20,** 1077 (1976).
14. G. S. Y. Yeh, *Polym. Eng. Sci.*, **16,** 138 (1976).
15. A. Peterlin, *Polym. Eng. Sci.*, **16,** 126 (1976).
16. P. J. Flory, *J. Chem. Phys.*, **15,** 397 (1947).
17. P. F. Dismore and W. O. Statton, *J. Polym. Sci. C,* **13,** 133 (1966).
18. B. J. A. M. Sprock, J. v. Soest, and I. M. C. v.d. Eijnden, unpublished results.

Received February 28, 1977